

Signature splitting, shape evolution, and nearly degenerate bands in  $^{108}\text{Ag}$ 

C. Liu (刘晨),<sup>1</sup> S. Y. Wang (王守宇),<sup>1,\*</sup> B. Qi (齐斌),<sup>1</sup> D. P. Sun (孙大鹏),<sup>1</sup> S. Wang (王硕),<sup>1</sup> C. J. Xu (徐长江),<sup>1</sup> L. Liu (刘雷),<sup>1</sup> P. Zhang (张盼),<sup>1</sup> Z. Q. Li (李志泉),<sup>1</sup> B. Wang (王彬),<sup>1</sup> X. C. Shen (沈晓晨),<sup>1</sup> M. R. Qin (秦慕容),<sup>1</sup> H. L. Liu (刘红亮),<sup>2</sup> Y. Gao (高原),<sup>3</sup> L. H. Zhu (竺礼华),<sup>4</sup> X. G. Wu (吴晓光),<sup>5</sup> G. S. Li (李广生),<sup>5</sup> C. Y. He (贺创业),<sup>5</sup> and Y. Zheng (郑云)<sup>5</sup>

<sup>1</sup>Shandong Provincial Key Laboratory of Optical Astronomy and Solar-Terrestrial Environment, School of Space Science and Physics, Shandong University, Weihai 264209, People's Republic of China

<sup>2</sup>Department of Applied Physics, Xi'an Jiaotong University, Xi'an 710049, People's Republic of China

<sup>3</sup>State Key Laboratory of Nuclear Physics and Technology, School of Physics, Peking University, Beijing 100871, People's Republic of China

<sup>4</sup>School of Physics and Nuclear Energy Engineering, Beihang University, Beijing 100191, People's Republic of China

<sup>5</sup>China Institute of Atomic Energy, Beijing 102413, People's Republic of China

(Received 31 July 2013; published 17 September 2013)

High spin states in  $^{108}\text{Ag}$  have been studied via in-beam  $\gamma$  spectroscopy techniques using the  $^{104}\text{Ru}(^7\text{Li}, 3n)$  reaction. The previously known level scheme has been extended, and a new band structure has been established. The configurations have been tentatively assigned to all observed rotational bands. The signature splitting behavior of the  $\pi g_{9/2} \otimes \nu g_{7/2}$  band has been discussed and interpreted as a change in shape from near-oblate to prolate. A systematic study of the nearly degenerate negative-parity bands in the  $A \sim 110$  mass region has been performed and it is found that the yrast band in  $^{108}\text{Ag}$  and its side band show different behaviors with those expected from a pair of chiral bands.

DOI: [10.1103/PhysRevC.88.037301](https://doi.org/10.1103/PhysRevC.88.037301)

PACS number(s): 27.60.+j, 21.60.-n, 23.20.Lv, 21.10.Re

High spin states of the odd-odd nuclei in the  $A \sim 110$  mass region have been extensively studied in recent years. In this mass region, the high- $\Omega$   $\pi g_{9/2}$  orbital drives the nuclei towards negative  $\gamma$  values, while the low- $\Omega$   $\nu h_{11/2}$  orbital drives the nuclei towards positive  $\gamma$  values. The delicate interplay of the high- $\Omega$   $\pi g_{9/2}$  and low- $\Omega$   $\nu h_{11/2}$  orbitals would influence the overall shape of the nucleus and result in  $\gamma$ -soft or triaxial shapes. Indeed, several interesting phenomena based on different deformations have been reported in this mass region such as signature inversion [1], shape evolution and coexistence [2], magnetic rotation [3], and chiral doublet bands [4,5].

For the odd-odd nucleus  $^{108}\text{Ag}$  with  $Z = 47$  and  $N = 61$ , the proton Fermi level lies near the top of the  $g_{9/2}$  subshell, while the neutron Fermi level lies at the  $h_{11/2}$ ,  $g_{7/2}$ ,  $d_{5/2}$ , or  $d_{3/2}$  subshells. The different quasiparticle configurations can drive  $^{108}\text{Ag}$  to form different shapes. Therefore, some interesting phenomena based on different shapes are expected to occur in  $^{108}\text{Ag}$ . Furthermore, it should be noted that  $^{108}\text{Ag}$  has two protons more than  $^{106}\text{Rh}$  and two neutrons more than  $^{106}\text{Ag}$ .  $^{106}\text{Rh}$  is usually regarded as the best known example of chiral nucleus in the  $A \sim 100$  mass region [6,7], whereas the observed doublet bands in  $^{106}\text{Ag}$  were interpreted as the coexistence of triaxial and axial shapes [8]. It is still unclear whether the nearly degenerate bands in  $^{108}\text{Ag}$  is associated with the nuclear chirality or the shape coexistence.

Based on the above consideration, experiments were performed to investigate structural features of the odd-odd nucleus  $^{108}\text{Ag}$  via in-beam  $\gamma$  spectroscopy techniques. Preliminary result of the present work was published in Ref. [9].

The  $^{104}\text{Ru}(^7\text{Li}, 3n)$  reaction at a beam energy of 33 MeV was used to populate the high spin states in  $^{108}\text{Ag}$ . The target

was an enriched  $^{104}\text{Ru}$  metallic foil of  $2 \text{ mg/cm}^2$  thickness with an evaporated  $10 \text{ mg/cm}^2$  Pb backing. The beam was provided by the HI-13 tandem accelerator of China Institute of Atomic Energy (CIAE). Deexcitation  $\gamma$  rays were detected using an array of 12 BGO suppressed HPGe detectors and a Clover detector. In this array, three HPGe detectors and the Clover detector were located at  $90^\circ$ , six HPGe detectors were located at  $\pm 40^\circ$  and three HPGe detectors were located at  $\pm 65^\circ$  with respect to the beam direction. A total of  $2 \times 10^8$   $\gamma$ - $\gamma$  coincidence events were collected. In the off-line analysis, the coincidence data were recalibrated to  $0.5 \text{ keV/channel}$  and sorted into a  $4096 \times 4096$  symmetrized matrix. To obtain information on the multipole order of  $\gamma$  rays, an asymmetric DCO (directional correlation ratios of oriented states) matrix was created by sorting the data from the detectors positioned at  $\sim \pm 40^\circ$  against the detectors at  $\sim 90^\circ$  with respect to the beam direction. For the present geometry, DCO ratio  $\sim 1.1$  is expected for the stretched quadrupole transitions and  $\sim 0.6$  for the pure stretched dipole ones by gating on the stretched quadrupole transitions.

The level scheme of  $^{108}\text{Ag}$  deduced from the present work is shown in Fig. 1. Seven band-like structures were observed and labeled 1–7 for the facility of discussions. This scheme was established on the basis of coincidence relationships, relative intensities and DCO ratios of the  $\gamma$  rays. Examples of typical gated  $\gamma$  spectra are shown in Fig. 2. As shown in Fig. 1, the level scheme is divided into two independent parts (positive- and negative-parity structures). We discuss them separately beginning with the positive-parity structures.

Preliminary results of bands 1 and 2 have been reported in Ref. [9]. Band 2 is directly based on the  $I^\pi = 6^+$  isomer and has been assigned to be the  $\pi g_{9/2} \otimes \nu d_{5/2}$  configuration [9]. In Ref. [9], band 1 has been extended and reassigned as the  $\pi g_{9/2} \otimes \nu g_{7/2}$  and  $\pi g_{9/2} \otimes \nu g_{7/2}(h_{11/2})^2$  configurations below and above the backbending, respectively. Based on the

\*sywang@sdu.edu.cn

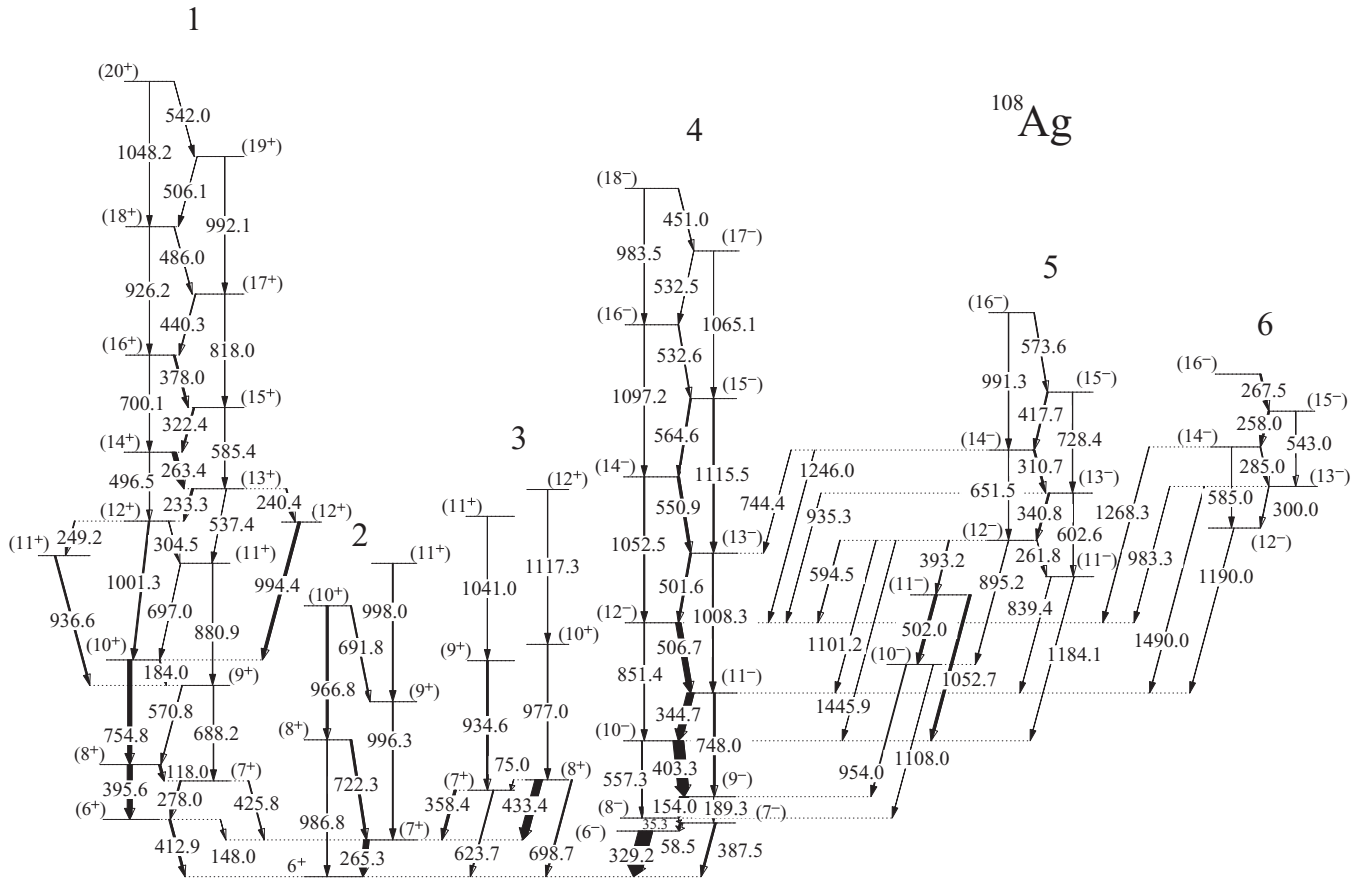


FIG. 1. Level scheme of  $^{108}\text{Ag}$  deduced from the present work. Transition energies are given in keV, while the widths of the arrows indicate their relative intensities.

configuration and spin-parity assignments given in Ref. [9], we analyzed the characteristics of signature splitting in band 1. The convention  $S(I) = E(I) - E(I-1) - [E(I+1) - E(I) + E(I-1) - E(I-2)]/2$  was used to display the signature splitting. The  $S(I)$  versus  $I$  are plotted in Fig. 3 for band 1 in  $^{108}\text{Ag}$  and the band with the same configuration in  $^{106}\text{Ag}$  [10]. One can see from Fig. 3 that the pattern of signature splitting for  $^{106}\text{Ag}$  and  $^{108}\text{Ag}$  are very similar. The signature splitting is large at low spins. After the alignment of a pair of  $h_{11/2}$  neutrons, the signature splitting reduces significantly, then an anomalous signature splitting (signature inversion) can be seen at high spins. The similar signature splitting behavior has been observed in many nuclei in the rare-earth region and interpreted as a change in shape from negative to zero or slightly positive values of  $\gamma$  [11]. The positive values of  $\gamma$  is able to cause signature inversion [12].

To gain a better understanding of the nuclear structure of  $^{108}\text{Ag}$ , total Routhian surface (TRS) cranking calculations [13,14] were performed. Selected examples of TRSs for  $\pi g_{9/2} \otimes \nu g_{7/2}$  configuration below and above the neutron alignment are presented in Fig. 4. The energy contours are at 200 keV intervals. As shown in Fig. 4, the TRS calculations show a minimum with  $\beta_2 = 0.11$  and  $\gamma = -48.8^\circ$  at rotational frequency  $\hbar\omega = 0.25$  MeV (below the neutron alignment), and this minimum is shifted toward  $\beta_2 = 0.17$  and  $\gamma = 6.6^\circ$

at a rotational frequency of  $\hbar\omega = 0.35$  MeV (above the neutron alignment). It means that band 1 in  $^{108}\text{Ag}$  undergoes a shape change, which is induced by the aligned  $h_{11/2}$  quasineutrons, from a near-oblate to prolate with increasing rotational frequency. The change in  $\gamma$  value from negative to slightly positive might be the cause for the reduction of the signature splitting and the observed signature inversion. The total Routhians for band 1 are calculated using the TRS deformations. The calculation results show that the signature splittings ( $\Delta e' = e'_{\text{unfavor}} - e'_{\text{favor}}$ ) are 51 keV and  $-40$  keV for  $\hbar\omega = 0.25$  MeV and  $\hbar\omega = 0.35$  MeV, respectively. It indicates that band 1 in  $^{108}\text{Ag}$  undergoes a signature inversion, which is consistent with the experimental observations.

Band 3 is a weakly populated band, which is linked to band 2 by four  $\gamma$  rays. The extracted DCO values for these linking transitions suggest that band 3 has the same parity (positive-parity) as band 2. It is consistent with the previous parity assignment given in Ref. [15]. The  $\nu g_{7/2}$  and  $\nu d_{5/2}$  orbitals have been occupied by bands 1 and 2, respectively. Thus, we tentatively adopt the  $\pi g_{9/2} \otimes \nu d_{3/2}$  configuration for band 3.

A particular interesting aspect of the present work is the observation of three nearly degenerate negative-parity bands (4, 5, and 6). Compared with the level scheme of Ref. [15], band 4 has been extended up to  $I^\pi = 18^-$ , three in-band

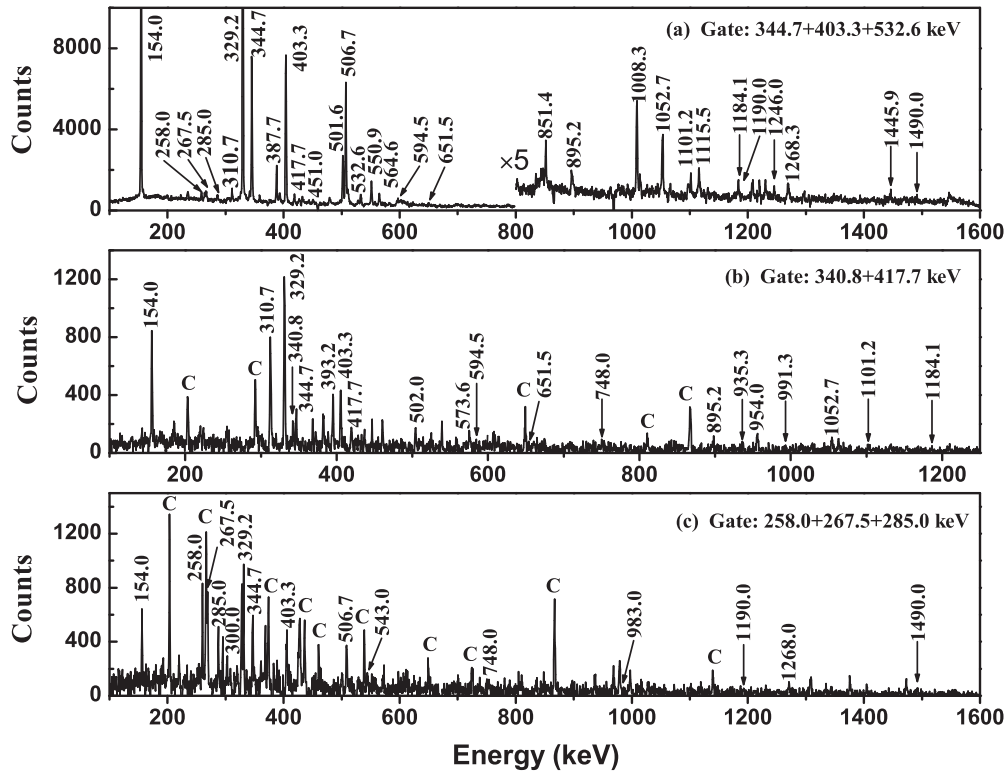


FIG. 2. Typical samples of  $\gamma$ -ray coincidence spectra in  $^{108}\text{Ag}$ . The peaks labeled C indicate contaminations.

quadrupole transitions (602.6, 651.5, and 728.4 keV) were added into band 5, and five new linking transitions (744.4, 839.4, 935.3, 1246.0, and 1445.9 keV) between bands 4 and 5 were identified. The present work has also confirmed the previous spin-parity assignments of bands 4 and 5 [15]. Band 6 is a newly observed rotational band, which feeds into band 4 via four linking transitions with energies of 983.3, 1190.0, 1268.3, and 1490.0 keV. The placements of band 6 were determined definitely according to these linking transitions, which could be weakly seen in Figs. 2(a) and 2(c). The DCO ratios of 1190.0 and 1268.3 keV transitions can be extracted. The extracted DCO ratios for 1190.0 and 1268.3 keV transitions are 0.60(12) and 0.89(23), respectively. It implies that the 1190.0 keV transition have  $\Delta I = 1$   $M1/E2$  or  $E1$  character, and 1268.3 keV transition have an  $E2$  multipolarity. We do not adopt the  $E1$  character for the 1190.0 keV transition

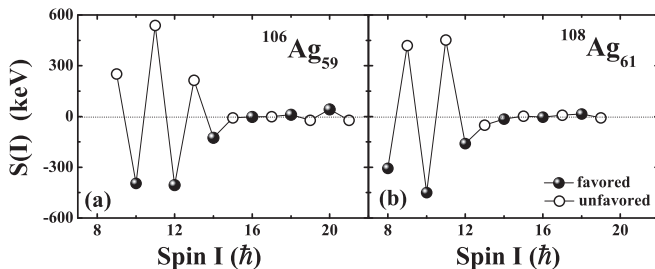


FIG. 3.  $S(I) = E(I) - E(I - 1) - [E(I + 1) - E(I) + E(I - 1) - E(I - 2)]/2$  for band 4 in  $^{108}\text{Ag}$  (present work) compared to the band with the same configuration in  $^{106}\text{Ag}$ .

because it would require an  $M2$  multipolarity for the 1268.3 keV transition, which would be highly unfavourable. Thus, the  $I^\pi = 12^-$  is tentatively assigned for the lowest observed state of band 6.

In Ref. [15], bands 4 and 5 have been assigned as the  $\pi g_{9/2} \otimes \nu h_{11/2}$  and  $\pi g_{9/2} \otimes \nu h_{11/2}(g_{7/2})^2$  configurations, respectively. Similar structures as bands 4 and 5 were also systematically observed in neighboring  $^{98,100}\text{Tc}$  [16,17],  $^{104,106}\text{Rh}$  [18,19], and  $^{106}\text{Ag}$  [8,10]. As mentioned in above, it is of particular interest to study the mechanism for the

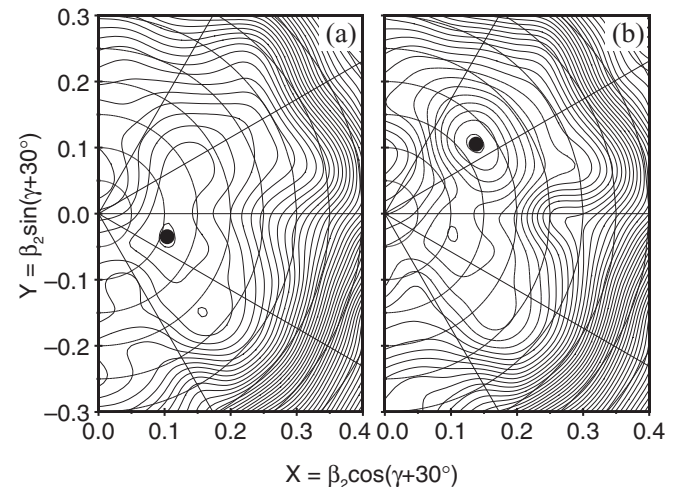


FIG. 4. TRS calculations for the  $\pi g_{9/2} \otimes \nu g_{7/2}$  configuration in  $^{108}\text{Ag}$  at rotational frequencies of 0.25 MeV and 0.35 MeV.

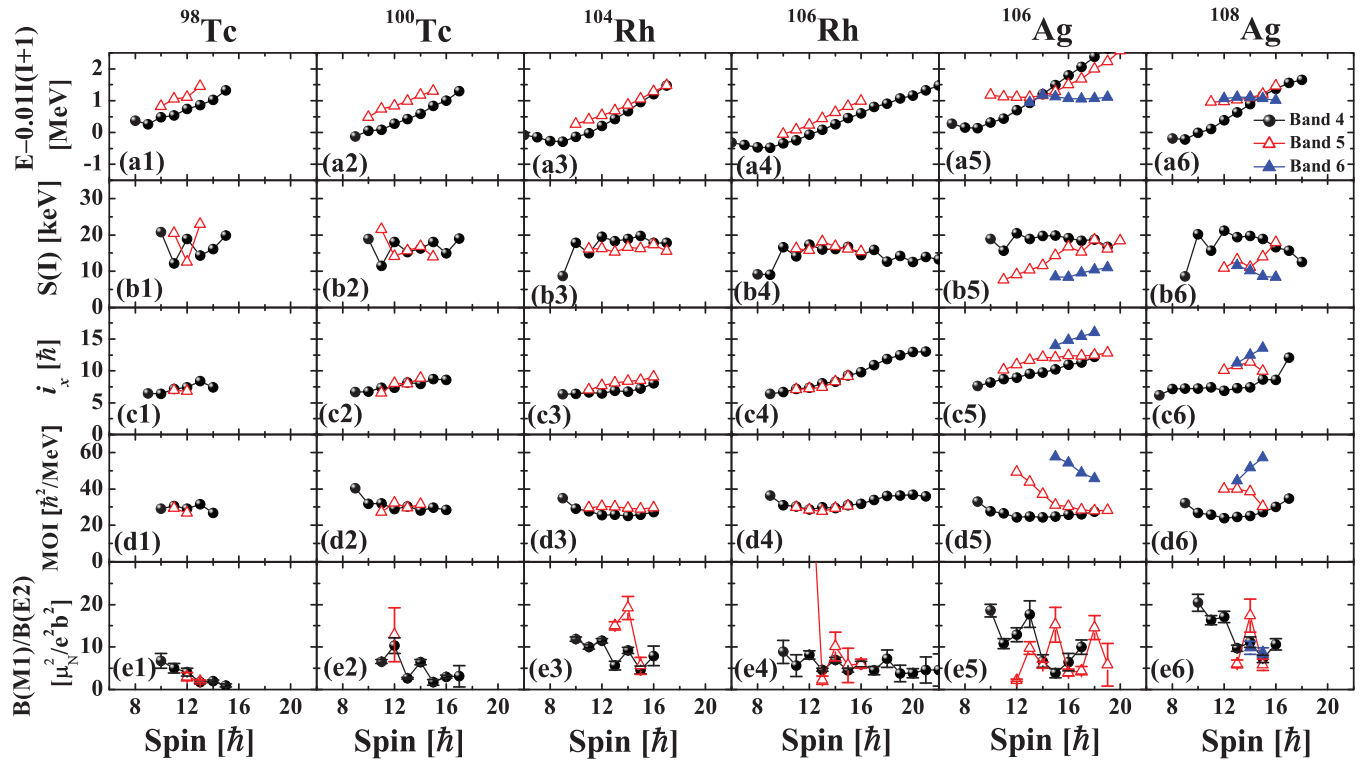


FIG. 5. (Color online) Excitation energies (a), the energy staggering parameter  $S(I) = [E(I) - E(I - 1)]/2I$  (b), experimental alignments (c), the kinematic moments of inertia (d), and experimental  $B(M1)/B(E2)$  ratios (e) as a function of spin for the nearly degenerate bands in  $^{98,100}\text{Tc}$  [16,17],  $^{104,106}\text{Rh}$  [18,19],  $^{106}\text{Ag}$  [8,10], and  $^{108}\text{Ag}$  (present work).

occurrence of the nearly degenerate bands in  $^{108}\text{Ag}$ . In order to discuss and compare the observed degenerate bands in  $^{108}\text{Ag}$  together with those in  $^{98,100}\text{Tc}$  [16,17],  $^{104,106}\text{Rh}$  [18,19], and  $^{106}\text{Ag}$  [8,10], the excitation energies, the energy staggering parameter  $S(I) = [E(I) - E(I - 1)]/2I$ , the experimental alignments ( $i_x$ ), the kinematic moments of inertia (MOI) and the  $B(M1)/B(E2)$  ratios for these bands are plotted in Fig. 5 as a function of spin. As shown in Fig. 5, doublet bands in  $^{106}\text{Rh}$  have small energy differences ( $\sim 300$  keV), smooth variation  $S(I)$ , almost identical  $i_x$ , MOI, and  $B(M1)/B(E2)$  ratios within the observed spin interval. These properties of the doublet bands in  $^{106}\text{Rh}$  agree well with the expected chiral criteria [7], which provides a good example of chirality. The nearly degenerate bands in  $^{98,100}\text{Tc}$  and  $^{104}\text{Rh}$  also show consistent behaviors with those expected from chiral doublet bands. However, the values of  $S(I)$ ,  $i_x$  and MOI for the doublet bands in  $^{106}\text{Ag}$  are quite different within the observed spin interval. These experimental observations show marked differences from the systematics expected of chiral doublet bands. The doublet bands were interpreted to have the identical single-particle configurations but corresponded to different shapes in Ref. [8]. As shown in Fig. 5, all observed properties of  $^{108}\text{Ag}$  have a very similar behavior to those of  $^{106}\text{Ag}$ . It implies that the doublet bands in  $^{108}\text{Ag}$  and  $^{106}\text{Ag}$  have a common origin, i.e., the same single-particle configurations but different shapes.

TRS calculations for the  $\pi g_{9/2} \otimes \nu h_{11/2}$  configuration in  $^{108}\text{Ag}$  are shown in Fig. 6 for two rotational frequencies 0.25 MeV and 0.35 MeV. The deformation parameters  $\beta_2 =$

0.16,  $\gamma = 3.4^\circ$  and  $\beta_2 = 0.16$ ,  $\gamma = 0.1^\circ$  are obtained from the present calculation corresponding to  $\hbar\omega = 0.25$  and 0.35 MeV, respectively. It indicates that the  $\pi g_{9/2} \otimes \nu h_{11/2}$  configuration in  $^{108}\text{Ag}$  have a nearly axially symmetric shape, which is not suitable for the construction of chiral doublet bands. Both empirical systematics and TRS calculations indicate that bands 4 and 5 in  $^{108}\text{Ag}$  would not be a pair of chiral bands.

As shown in Fig. 5, new observed band 6 in  $^{108}\text{Ag}$  has the large alignment and the high excitation energy compared

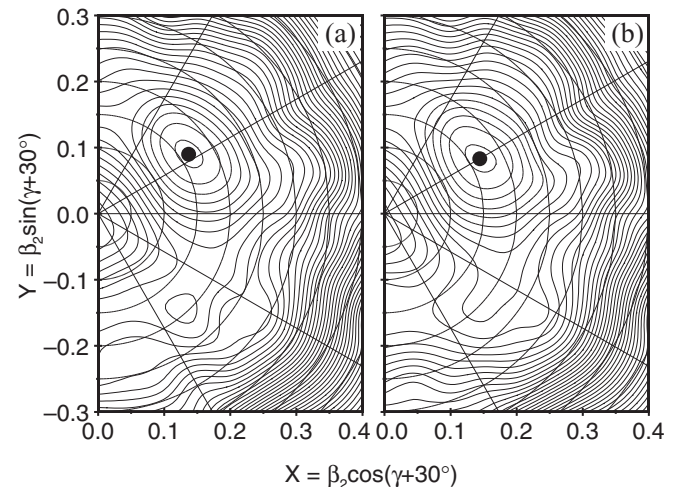


FIG. 6. TRS calculations for the  $\pi g_{9/2} \otimes \nu h_{11/2}$  configuration in  $^{108}\text{Ag}$  at rotational frequencies of 0.25 and 0.35 MeV.

with the yrast band, which indicates that band 6 is likely to be built on the four-quasiparticle configuration. We tentatively assigned  $\pi g_{9/2} \otimes \nu h_{11/2}(g_{7/2}, d_{5/2})^2$  configuration to band 6. Bands with the same configuration have already been reported in the neighboring odd-odd nuclei  $^{108,110}\text{In}$  [20] and  $^{106}\text{Ag}$  [10]. This provides further support for the present configuration assignment of band 6.

During the preparation of the present manuscript, another work [21] was published and which suggest that the doublet bands (labeled 4 and 5 in the present work) in  $^{108}\text{Ag}$  originate from two different quasiparticle structures.

In summary, high spin states in  $^{108}\text{Ag}$  have been studied via the  $^{104}\text{Ru}(^7\text{Li}, 3n)$  reaction at the beam energy of 33 MeV. The previous reported level scheme has been confirmed and extended, and a new band structure has been established. The configurations have been tentatively assigned to all observed rotational bands. The signature inversion was observed in the

$\pi g_{9/2} \otimes \nu g_{7/2}$  band and this phenomenon was interpreted as a change in shape from near-oblate to prolate. A systematic study of the nearly degenerate negative-parity bands in the  $A \sim 110$  mass region has been performed and it is found that the yrast band in  $^{108}\text{Ag}$  and its side band show different behaviors with those expected from a pair of chiral bands.

The authors express their gratitude to Professor F. R. Xu for providing the deformation calculation. This work is supported by the National Natural Science Foundation (Grant Nos. 11175108 and 11005069), the Shandong Natural Science Foundation (Grant No. ZR2010AQ005), the Independent Innovation Foundation of Shandong University IIFSDU (Nos. 2013ZRYQ001 and 2011ZRYQ004), and the Graduate Innovation Foundation of Shandong University at WeiHai GIFSDUWH (No. yjs11031) of China.

- 
- [1] J. Timár *et al.*, *Acta Phys. Pol. B* **33**, 493 (2002).  
 [2] K. Heyde and J. L. Wood, *Rev. Mod. Phys.* **83**, 1467 (2011).  
 [3] H. Hübel, *Prog. Part. Nucl. Phys.* **54**, 1 (2005).  
 [4] S. Frauendorf and J. Meng, *Nucl. Phys. A* **617**, 131 (1997).  
 [5] J. Meng and S. Q. Zhang, *J. Phys. G* **37**, 064025 (2010).  
 [6] S. Y. Wang, S. Q. Zhang, B. Qi, J. Peng, Y. M. Yao, and J. Meng, *Phys. Rev. C* **77**, 034314 (2008).  
 [7] S. Y. Wang, S. Q. Zhang, B. Qi, and J. Meng, *Chin. Phys. Lett.* **24**, 664 (2007).  
 [8] P. Joshi, M. P. Carpenter, D. B. Fossan, T. Koike, E. S. Paul, G. Rainovski, K. Starosta, C. Vaman, and R. Wadsworth, *Phys. Rev. Lett.* **98**, 102501 (2007).  
 [9] C. Liu *et al.*, *Int. J. Mod. Phys. E* **20**, 2351 (2011).  
 [10] C. Y. He *et al.*, *Phys. Rev. C* **81**, 057301 (2010).  
 [11] S. Frauendorf and F. R. May, *Phys. Lett. B* **125**, 245 (1983).  
 [12] R. Bengtsson, J. A. Pinston, D. Barneoud, E. Monnard, and F. Schussler, *Nucl. Phys. A* **389**, 158 (1982).  
 [13] W. Satula, R. Wyss, and P. Magierski, *Nucl. Phys. A* **578**, 45 (1994).  
 [14] F. R. Xu, W. Satula, and R. Wyss, *Nucl. Phys. A* **669**, 119 (2000).  
 [15] F. R. Espinoza-Quiñones *et al.*, *Phys. Rev. C* **52**, 104 (1995).  
 [16] H. B. Ding *et al.*, *Chin. Phys. Lett.* **27**, 072501 (2010).  
 [17] P. Joshi *et al.*, *Eur. Phys. J. A* **24**, 23 (2005).  
 [18] C. Vaman, D. B. Fossan, T. Koike, K. Starosta, I. Y. Lee, and A. O. Macchiavelli, *Phys. Rev. Lett.* **92**, 032501 (2004).  
 [19] P. Joshi *et al.*, *Phys. Lett. B* **595**, 135 (2004).  
 [20] C. J. Chiara *et al.*, *Phys. Rev. C* **64**, 054314 (2001).  
 [21] J. Sethi *et al.*, *Phys. Lett. B* **725**, 85 (2013).